Quantum spinodal phenomena

Seiji Miyashita*
Department of Physics, Graduate School of Science, The University of Tokyo, 7-3-1 Hongo, Bunkyo-Ku, Tokyo 113-8656, Japan and CREST, JST, 4-1-8 Honcho Kawaguchi, Saitama 332-0012, Japan

Hans De Raedt
Department of Applied Physics, Zernike Institute of Advanced Materials, University of Groningen, Nijenborgh 4, NL-9747 AG Groningen, The Netherlands

Bernard Barbara
Institut Néel, CNRS, 25 Ave. des Martyrs, BP 166, 38 042 Grenoble Cedex 09, France
(Received 27 November 2008; published 20 March 2009)

We study the dynamical magnetization process in the ordered ground-state phase of the transverse Ising model under sweeps of magnetic field with constant velocities. In the case of very slow sweeps and for small systems studied previously [H. De Raedt *et al.*, Phys. Rev. B **56**, 11761 (1997)], nonadiabatic transitions at avoided level-crossing points give the dominant contribution to the shape of magnetization process. In contrast, in the ordered phase of this model and for fast sweeps, we find significant size-independent jumps in the magnetization process. We study this phenomenon in analogy to the spinodal decomposition in classical ordered state and investigate its properties and its dependence on the system parameters. An attempt to understand the magnetization dynamics under field sweep in terms of the energy-level structure is made. We discuss a microscopic mechanism of magnetization dynamics from a viewpoint of local cluster flips and show that this provides a picture that explains the size independence. The magnetization dynamics in the fast-sweep regime is studied by perturbation theory and we present a perturbation scheme based on interacting Landau-Zener-type processes to describe the local cluster flip dynamics.

DOI: 10.1103/PhysRevB.79.104422 PACS number(s): 75.10.Jm, 75.50.Xx, 75.45.+j, 75.60.Jk

I. INTRODUCTION

It is well known that nonadiabatic transitions among adiabatic eigenstates take place when an external field is swept with finite velocity.[1,2] In particular, at avoided level-crossing points strong nonadiabatic transitions occur, causing a stepwise magnetization process.[3]

In the so-called single-molecule magnets,[4] the energy-level diagram consists of discrete levels because the molecules contain only small number of magnetic ions and hence the quantum dynamics plays an important role. In particular, in the easy-axis large spin molecules such as Mn_{12} and Fe_8, stepwise magnetization processes have been found and they are attributed to the adiabatic change—that is, the quantum tunneling at the avoided level-crossing points—and are called resonant tunneling phenomena.[5] The Landau-Zener (LZ) mechanism also causes various interesting magnetization loops in field cycling processes.[6]

The amount of the change in the magnetization at a step in the magnetization process is governed by the Landau-Zener mechanism and depends significantly on the energy gap at the crossing. This dependence has played an important role in the study of single-molecule magnets. Observations of the gap have been done on isolated magnetic molecules.[7]

The quantum dynamics of systems of strongly interacting systems which show quantum phase transitions is also of much contemporary interest. As far as static properties are concerned, the action in the path-integral representation of a d-dimensional quantum system maps onto the partition function of a $(d+1)$-dimensional classical model, which is the key ingredient of the quantum Monte Carlo simulation.[8] From this mapping, it follows that the critical properties of the ground state of the d-dimensional quantum system are the same as those of the equilibrium state of the $(d+1)$-dimensional classical model, with quantum fluctuations playing the role of the thermal fluctuations at finite temperatures.

However, from a viewpoint of dynamics, the nature of the quantum and thermal fluctuations is not necessarily the same. Thus, it is of interest to study dynamical aspects of quantum critical phenomena. As a typical model showing quantum critical phenomena, in the present work we adopt the one-dimensional transverse Ising model.[9]

Recently, interesting properties of molecular chains which are modeled by the transverse Ising model with large spins have been reported.[10] However, in this paper, we focus ourselves to systems of $S=1/2$. The dynamics of the transverse Ising model plays an important role in the study of quantum annealing in which the quantum fluctuations due to the transverse field are used to survey the ground state in a complex system.[11] The dynamics of domain growth under the sweep of the transverse field through the critical point has been studied in relation to the Kibble-Zurek mechanism.[12,13]

In this paper, we study the hysteresis behavior as a function of the external field in the ordered state by performing simulations of pure quantum dynamics—that is, by solving the time-dependent Schrödinger equation.[14] This gives us numerically exact results of the dynamical magnetization process of the transverse Ising model under sweeps of magnetic field with constant velocities.

Previously we have studied the time evolution of magnetization of the transverse Ising model from a viewpoint of

Landau-Zener transition, sweeping the field slowly and finding transitions at each avoided level-crossing point.[3] However, for fast sweeps the transition at zero field $H_z=0$ disappears and the magnetization does not change even after the field reverses. The magnetization remains in the direction opposite to the external field for a while, and when the magnetic field reaches a certain value, the magnetization suddenly changes to the direction of the field. This sudden change is also found for very slow sweeps at the level-crossing point. However, the present case has the following two differences: (1) the switching field does not necessarily correspond to a level crossing and (2) in all cases the changes are independent of the size L of the system. This sudden change resembles the change in magnetization at the coercive field in the hysteresis loop of ferromagnetic systems, where it is called spinodal decomposition. Therefore, we will call the phenomenon that we observe in the quantum system a "quantum spinodal decomposition" and the field "quantum spinodal point" H_{SP}. We study the dependence of H_{SP} on the transverse field H_x and also study the sweep-velocity dependence of H_{SP}.

As in the case of the single-molecule magnets, it should be possible to understand the dynamics of the magnetization in terms of the energy levels as a function of field. However, because the structure of the energy-level diagram strongly depends on the size of the system, it is difficult to explain the size-independent property of the quantum spinodal decomposition from the energy-level structure only. In the case of much faster sweeps, we find almost perfect size-independent magnetization processes. We also find a peculiar dependence of magnetization on the field in the case of weak transverse fields. These processes can be understood from the energy-level diagram for local flips of spins, but not from the energy diagram of the total system.

In this paper, we attempt to understand the microscopic mechanism that gives rise to this size-independent dynamics. We present a perturbation scheme for fast sweeps, regarding the fast-sweeping field term as the unperturbed system and treating the interaction term as the perturbation. From this viewpoint, we investigate fundamental spatially-local time evolutions which yield the size-independent response to the sweep procedure. In particular, we propose a perturbation scheme in terms of independent Landau-Zener systems, each of which consists of a spin in a transverse and sweeping field. A system consisting of locally interacting Landau-Zener systems explains well the magnetization dynamics for fast sweeps.

II. MODEL

We study characteristics of dynamics of the order parameter of the one-dimensional transverse Ising model with periodic boundary condition under a sweeping field.[9] The Hamiltonian of the system is given by

$$\mathcal{H}(t) = -J\sum_i \sigma_i^z\sigma_{i+1}^z - H_x\sum_i \sigma_i^x - H_z(t)\sum_i \sigma_i^z, \qquad (1)$$

where σ_i^x and σ_i^z are the x and z components of the Pauli matrix, respectively. Hereafter, we take J as a unit of the energy. The order parameter is the z component of the magnetization

$$M^z = \sum_i \sigma_i^z. \qquad (2)$$

We study the dynamics of the order parameter of the model, i.e., the time dependence of the magnetization under the time-dependent field $H_z(t)$,

$$\langle M^z\rangle = \langle\Psi(t)|M^z|\Psi(t)\rangle, \qquad (3)$$

where $|\Psi(t)\rangle$ is a time-dependent wave function given by the Schrödinger equation

$$i\hbar\frac{\partial}{\partial t}|\Psi(t)\rangle = \mathcal{H}(t)|\Psi(t)\rangle. \qquad (4)$$

In the present paper we study the case of linear sweep of the field

$$H_z(t) = -H_0 + ct, \qquad (5)$$

where $-H_0$ is an initial magnetic field. In the present paper, we set $H_0/J=1$ and c is the speed of the sweep. We use a unit where $\hbar=1$.

In the case $H_z=0$, the model shows an order-disorder phase transition as a function of H_x. The transition point is given by $H_x^c=J$. In the ordered phase ($H_x<J$), the system has a spontaneous magnetization m_s,

$$m_s = \lim_{H_z\to+0}\lim_{L\to\infty}\langle G(0)|M^z|G(0)\rangle, \qquad (6)$$

where $|G(0)\rangle$ is the ground state of the model with $H_z=0$. Therefore, the ground state is twofold degenerate with symmetry-broken magnetization, while the ground state is unique when $H_x>J$. Because of these twofold symmetry-broken ground states, the magnetization changes discontinuously at $H_z=0$.

In a finite system $L<\infty$, this degeneracy is resolved by the quantum mixing (tunneling effect) and a small gap opens at $H_z=0$. This gap becomes small exponentially with L as shown in Appendix A. Therefore, the change in the magnetization becomes sharper as L increases. Dynamical realization of this change by field sweeping becomes increasingly difficult with L. This phenomenon corresponds to the existence of a metastable state.

The energy-level diagram becomes complicated when L increases. However, as shown below, when c is large the system shows a size-independent magnetization dynamics which is not easily understood in terms of the energy-level diagram. In this paper, we focus on the regime of moderate to large sweep velocities.

III. ENERGY STRUCTURE

In Fig. 1(a), we present an energy-level diagram for $L=6$ and $H_x=0.7$. We plot all energy levels as a function of H_z. We find that the energy levels show a linear dependence at large fields, where quantum fluctuations due to H_x have little effect. The levels are mixed in the region $-3<H_z/J<3$ where the energy levels come close and are mixed by the

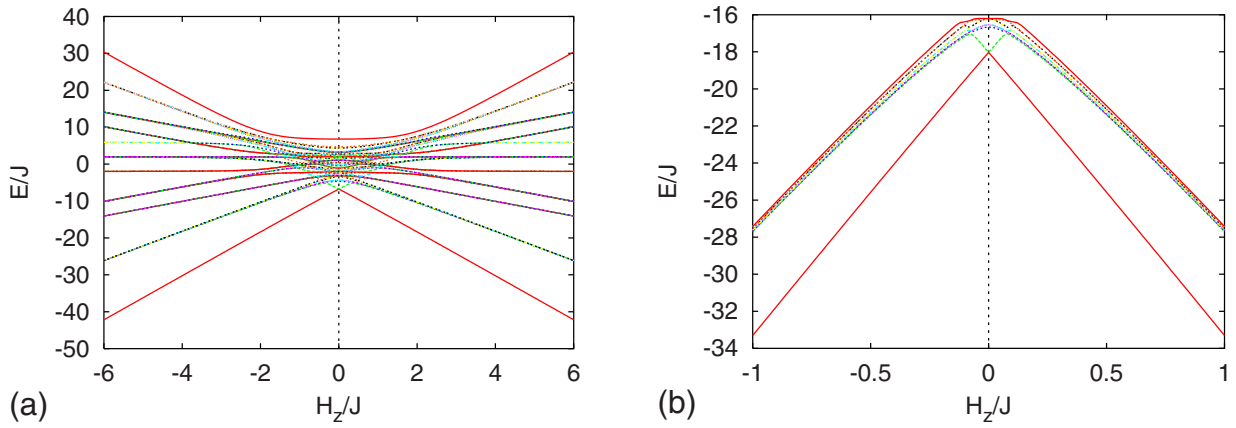

FIG. 1. (Color online) Typical energy-level diagrams of model (1). (a) Full spectrum for $L=6, H_x=0.7$. (b) A few low-energy states for $L=16, H_x=0.7$.

transverse field. The isolated two lowest-energy levels are located under a densely mixed area, which represent the ordered states with $M=L$ and $-L$, and they cross at $H_z=0$ with a small gap ΔE_1, reflecting the tunneling between the symmetry-broken states. The gap ΔE_1 is so small that one cannot see it in Fig. 1(a). After the crossing, these states join the densely mixed area. In Fig. 1(b), we show the energy levels for $L=16$ where we plot only energies of a few low-energy states. In this figure, we also find the above-mentioned characteristic structure of two lowest-energy levels.

Let us point out a few more characteristic features of the energy-level diagram. A finite gap ΔE_2 exists between the crossing point of the low-lying lines and the densely populated region of excited states. The d-dimensional Ising model in a transverse field is closely related to the transfer matrix of $(d+1)$-dimensional Ising model. From this analogy, we associate ΔE_1 to symmetry-breaking phenomena. When symmetry-breaking takes place, the two largest eigenvalues of the transfer matrix of the model become almost degenerate. The energy gap corresponds to the tunneling through the free-energy barrier between the two ordered states and vanishes exponentially with the system size. On the other hand, ΔE_2 is related to the correlation length of the fluctuation of antiparallel domains in the ordered state. The correlation length is finite at a given temperature in the ordered state and is almost size independent. At $H_z=0$ we can calculate eigenenergies analytically and we can explicitly confirm that ΔE_1 vanishes exponentially with L and that ΔE_2 is almost constant as a function of the size. The dependencies of the energy gaps at $H_z=0$ are discussed in Appendix A.

For large H_z, the slopes of the low-lying isolated lines are $\pm L$ because they represent the states with $M=\pm L$. Thus, the field at which the lines merge in the area of densely populated excited states is given by

$$H_z \simeq \frac{\Delta E_2}{L} \equiv H_z^*(L). \tag{7}$$

At this point, the magnetization shows a jump when the speed of the sweep is very slow.[3]

However, as we will see in Sec. IV, the dynamical magnetization does not show any significant change at this field value when the sweeping field is fast. Another type of jump which we called quantum spinodal jump or quantum spinodal transition will occur.

IV. EVOLUTION OF THE MAGNETIZATION FOR FAST SWEEPS OF THE FIELD

A. Quantum spinodal decomposition

When we sweep the magnetic field from $H_z=-1$ to $H_z=1$, the magnetization shows a rapid increase to a positive value. In Fig. 2, we depict examples of dynamics of the magnetization as a function of time for a sweeping velocity $c=0.001$. Because $H_z(t)=-H_0+ct$, H_z also represents time.

The magnetization stays at a negative value until a certain field strength is reached. The system can be regarded as being in a metastable state. Then, the magnetization changes significantly toward the direction of the field in a single continuous jump, with the magnetization processes $M_z(t)$ depending very weakly on the system size. In the classical ordered state, we know a similar behavior. Namely, at the coercive field (at the edge of the hysteresis), the magnetization relaxes very fast and the relaxation time does not depend on the size. Thus, we may make an analogy to the spinodal decomposition phenomena. We call the phenomenon that we observe in the quantum system quantum spinodal decomposition and we call the field at which the magnetization changes H_{SP}. It should be noted that the spinodal decomposition corresponds to the fact that the size of the critical nuclei becomes of the order 1. If the size of the critical nuclei is larger than the size of the particle, as in the case of nanoparticles, the critical field of the sudden magnetization reversal, which is also a kind of spinodal decomposition, strongly depends on the size.

Let us attempt to understand this dynamics from the viewpoint of the energy diagram. As we mentioned in Sec. III, the low-lying levels of $M=\pm L$ merge with the continuum at $H_z=H_z^*$. Thus, we expect that at this point the magnetization begins to change because the states with $M=\pm L$ begin to cross other states. In fact, in earlier work, we found stepwise

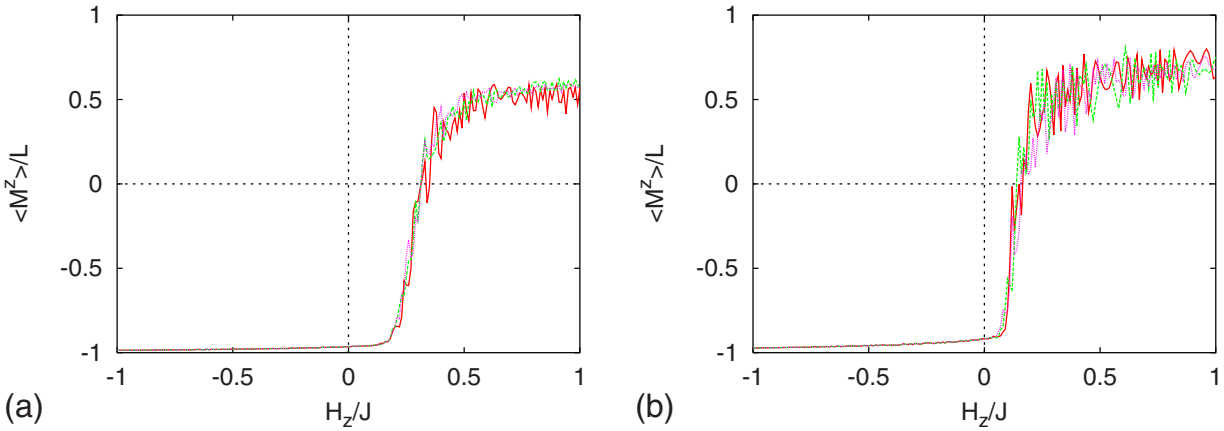

FIG. 2. (Color online) (a) Magnetization $M^z(t)$ as a function of $H_z(t)$ for $c=0.001$, $H_x=0.5$, and various system sizes. Solid (red) line: $L=12$; dashed (green) line: $L=14$; and dotted (magenta) line: $L=16$. (b) Same as (a) except that $H_x=0.7$. (Lines for different L overlap.)

magnetization processes at avoided level crossings in very slow sweeps, each of which could be analyzed in terms of successive Landau-Zener crossings.[3]

From Fig. 2(a), we find that the sharp change in $M_z(t)$ starts at $H_z=0.2-0.25$, which is much larger than $H_z^*(L)$. We estimate $H_z^*(12)\simeq 0.18$, and for larger lattices $H_z^*(L)$ is even smaller. Moreover, it should be noted that the magnetization processes display almost no size dependence. In Fig. 2(b), which shows $M_z(t)$ for $H_x=0.7$, we also find that the magnetization processes $M_z(t)$ for all sizes L are very similar. Here $H_{\rm SP}\approx 0.11$ is again significantly larger than $H_z^*(L)$ [for $L=16$ and $\Delta E_2\approx 1.4$ in the case $H_x=0.7$, and hence $H_z^*(14)\simeq 0.09$]. This observation is in conflict with the picture based on the structure of the energy-level diagram given earlier.

In Fig. 3, we present an example of sweep-velocity dependence for a system with $L=20$ (results of other sizes are not shown). The magnetization processes show strong dependence on the sweep velocity c, as expected. However, for fixed c, there is little dependence on L (results of other sizes are not shown).

We have found the characteristic change in the cases of relatively large quantum fluctuations, i.e., $H_x=0.5$ and 0.7. The size independence indicates that the change occurs locally. When H_x is small, the quantum fluctuations are weak and local flips of clusters consisting of small number of spins become dominant. In Fig. 4, $M^z(t)$ for $H_x=0.1$ is shown, where a peculiar sequence of jumps is found. It is almost independent of the system size (except for $L=2$). Before the large jump of the magnetization at $H_z/J=1$, there is a small but nonzero precursor jump around $H_z\simeq 2/3$. After these jumps, the magnetization shows a plateau of $M^z(t)/L\approx -1/2$ until the smooth crossover to the saturated value takes place around $H_z/J=2$. The value $H_z/J=2$ corresponds to the spinodal point of the corresponding classical model.

The positions of these jumps can be understood from the viewpoint of local "cluster" flips. Let us consider a single-spin flip—that is, a flip from the state with all spins $|--------\cdots\rangle$ to a state $|---+---\cdots\rangle$. The diabatic energies of these states are $E_0=-LJ+LH_z$ and $E_1=-(L-4)J-(L-2)H_z$, respectively. Thus, the crossing of these states occurs at $H_z^{(1)}=4J/2=2J$. The transition probability due to the transverse field H_x at this crossing is proportional to H_x^2

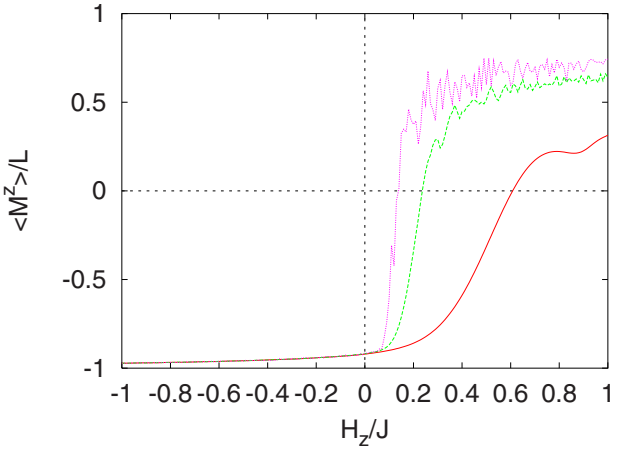

FIG. 3. (Color online) Magnetization $M^z(t)$ as a function of $H_z(t)$ for $L=20$ and $H_x=0.7$ and various sweep velocities. Solid (red) line: $c=0.1$; dashed (green) line: $c=0.01$; and dotted (magenta) line: $c=0.001$.

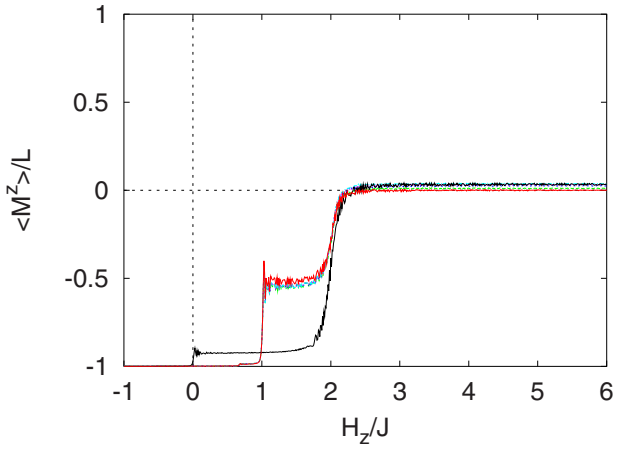

FIG. 4. (Color online) Magnetization $M^z(t)$ as a function of $H_z(t)$ for $H_x=0.1$, $c=0.001$, and various system sizes. Solid (black) line: $L=2$, showing a jump at $H_z=0$ and a plateau; solid (red) line: $L=4$, showing a spike; long dashed (green) line: $L=6$; dashed (magenta) line: $L=8$; dotted (red) line: $L=10$; and dashed dotted (blue) line: $L=12$. Curves for $L=6$, 8, 10, and 12 almost overlap.

because the matrix element for a single flip is proportional to H_x.

If we consider a collective flip of a connected cluster of m spins, the diabatic energy of this state is

$$E_m = -(L-4)J + (L-2m)H_z, \tag{8}$$

and thus the crossing of the states occurs at

$$H_z^{(m)} = 4J/2m = 2J/m. \tag{9}$$

For $m=2,3,\ldots$ we have $H_z^{(m)}=1,2/3,\ldots$, respectively. These values do not depend on L. It should be noted that, for the system $L=2$, the two-spin cluster ($m=2$) surrounded by + spins cannot be realized and no jump appears at $H_z/J=1$.

The matrix element for the m-spin cluster flip is proportional to H_x^m (see Appendix A). Therefore, for small H_x, only the flips with small values of m are appreciable. In the case of $H_x/J=0.1$ for $c=0.001$, jumps for $m \leq 2$ are observed. The change in the magnetization of each spin is given by a perturbation series and is independent of L as shown in Appendix B. These local flips may correspond to the nucleation in classical dynamics in metastable state.

If c becomes small or H_x becomes large, contributions from large values of m become relevant. Then, magnetization process consists of many jumps and amount of the change becomes large. But, as long as the perturbation series converges, we have a size-independent magnetization process, as shown in Fig. 2. This sharp and size-independent nature is consistent with the property of the classical spinodal decomposition.

In the classical system, the magnetization relaxes to its equilibrium value at the spinodal decomposition point. In contrast, for pure quantum dynamics, the magnetization of the state does not change for adiabatic motion along a particular energy level. Only if we include an effect of contact with the thermal bath, relaxation to the ground state takes place.[15]

Phase diagram

In Fig. 5, we give a schematic picture of the order parameter M as a function of the temperature T and the field H_z in the thermal phase transition of a ferromagnetic system. The overhanging structure signals the existence of the metastable state. The spinodal point is at the edge of the metastable branch. In this figure, the magnetic field is swept from positive to negative and the metastable positive magnetization jump down to the equilibrium value at $H_{\mathrm{SP}}(T)$.

In a mean-field theory for the magnetic phase transition at a finite temperature, the spinodal point is given by

$$H_{\mathrm{SP}} = -Jz\sqrt{1-\frac{k_BT}{J}} + \frac{k_BT}{2}\ln\left(\frac{1+\sqrt{1-\frac{k_BT}{J}}}{1-\sqrt{1-\frac{k_BT}{J}}}\right), \tag{10}$$

where z is the number of nearest-neighbor sites. We show the dependence of H_{SP} as a function of T by a dashed-dotted curve in Fig. 5.

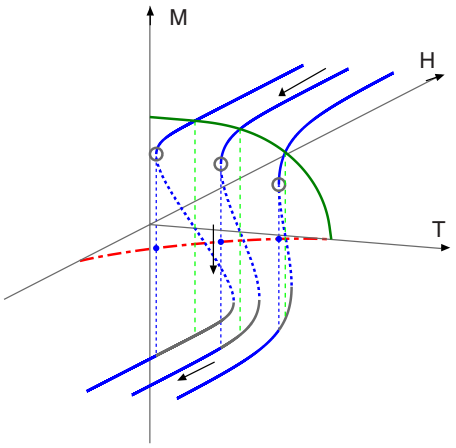

FIG. 5. (Color online) Schematic picture of the magnetization M as a function of field H below the critical temperature. Open circles denote the spinodal decomposition points. The (red) dashed-dotted curve in the H-T plane shows $H_{\mathrm{SP}}(T)$ as given by Eq. (10).

A similar argument can be made for the classical ground-state energy. Let the z component of spin be denoted by σ. Then, the energy is expressed by

$$E = -J\sigma^2 - H_x\sqrt{1-\sigma^2} - H\sigma. \tag{11}$$

We assume that the energy satisfies the condition

$$\frac{dE}{d\sigma} = 0, \tag{12}$$

which gives

$$-2J\sigma + \frac{H_x\sigma}{\sqrt{1-\sigma^2}} - H = 0. \tag{13}$$

Here, we consider the metastable state and thus we set $H=-|H|$ for $\sigma>0$. At the endpoint of metastability,

$$\frac{d\sigma}{dH} = \infty \quad \text{or} \quad \frac{dH}{d\sigma} = 0. \tag{14}$$

This leads to

$$\sigma = \left[1-\left(\frac{H_x}{2J}\right)^{2/3}\right]^{1/2}. \tag{15}$$

The endpoint of the metastable state is given by

$$H_{\mathrm{SP}} = 2J\left[1-\left(\frac{H_x}{2J}\right)^{2/3}\right]^{3/2}, \tag{16}$$

which gives H_{SP} as a function of H_x and is shown in Fig. 6 as the dotted curve.

It is interesting to note that expression (16) is very similar to the well-known expression of the Stoner-Wohlfarth model[16] for the reversal of a classical magnetic moment under the application of a magnetic field tilted with respect to the easy anisotropy axis. This is not surprising because, with both longitudinal and transverse field components, this model can be considered as a realization of the classical spinodal transition. One might derive the Stoner-Wohlfarth model from Eq. (11) by replacing the exchange energy pa-

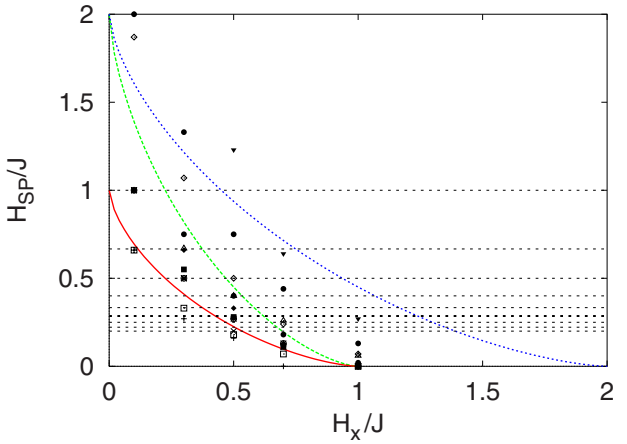

FIG. 6. (Color online) Spinodal points H_z^{SP} as a function of the quantum fluctuation H_x for various sweep velocities c. The horizontal dotted lines correspond to $2/m$ for $m=2,\ldots,10$ [see Eq. (9)]. Plus signs (1), crosses (2), and stars (3): $c=0.0001$; open squares (1), solid squares (2), and solid diamonds (3): $c=0.001$; open circles (1), bullets (2), and open diamonds (3): $c=0.01$; and open triangles (1), solid triangles (2), and inverted solid triangles (3): $c=0.1$. The numbers (1), (2), and (3) correspond to the field at which $M(t)$ shows a small but clear jump, $M(t)/L=-1/2$, and $M(t)$ saturates as a function of H_z, respectively. Dotted (blue) curve: The spinodal field H_{SP} according to Eq. (16); dashed (green) and solid (red) rescaled spinodal field (see text).

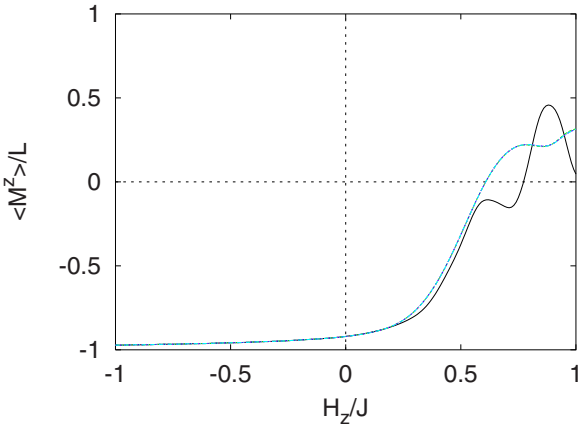

FIG. 7. (Color online) The magnetization $M(t)$ as a function of the sweeping field H_z for $H_x=0.7$, $c=0.1$, and various system sizes. Solid (black) line: $L=6$; solid (red) line: $L=14$; long dashed (green) line: $L=16$; dashed (magenta) line: $L=18$; dotted (red) line: $L=20$; and dashed dotted (blue) line: $L=12$. Except for $L=6$, all other curves overlap, indicating that for sufficiently large systems, the dependence on L is very weak. The curves for $L=12$, 14, 16, and 18 overlap and are difficult to distinguish.

rameter J with the anisotropy energy constant D.

It should be noted that the critical H_x is a factor of 2 larger than that of the correct value $H_c^x=J$ for the one-dimensional quantum model. This difference is due to the presence of quantum fluctuations. Therefore, in Fig. 6 we plot Eq. (16) with and without renormalized values of the fields. The dashed curve denotes the case of H_x scaled by 1/2 and the solid curve denotes the case where both H_x and H_z are scaled by 1/2.

As we saw in Fig. 2, we find a large change in magnetization at values of H_z for each value of H_x, which we called H_{SP}. In Fig. 6, we plot values of H_z at which: (1) $M(t)$ shows a small but clear jump, (2) $M(t)/L$ is equal to $-1/2$, and (3) $M(t)$ saturates as a function of H_z, for various values of c. The data show a dependence on H_x that shows a similar dependence to the dotted line. If we use other value of c, the values of H_z change. Although the values of H_z for (1)–(3) for larger values of c are larger than those for $c=0.001$, the values of H_z for $c=0.0001$ are close to those for $c=0.001$. They seem to saturate around the value of the dotted line and we may identify a sudden appearance of size-independent change as an indication for a quantum spinodal point. If we sweep much faster, the jumps of the magnetization become less clear, as we now study in more detail.

B. Very fast sweeps

For a fast sweep $c=0.1$, the magnetization processes for different sizes almost overlap each other (see Fig. 7). The data for $L=12$, 14, 16, and 20 are hard to distinguish. This almost perfect overlap is rather surprising from the viewpoint of the structure of energy-level diagram. The data for $L=6$ deviate from the others. This fact indicates that for these parameters ($H_x=0.7$, $c=0.1$) the relevant size of the cluster [m in Eq. (8)] is larger than 6 but smaller than 12.

Let us now study the behavior if we sweep much faster. In Fig. 8(a), we show the magnetization as a function of t [or $H_z(t)$] for $L=12$ with $c=10$, 20, 50, 100, and 200. For these parameters, the data for other L are almost indistinguishable from the $L=12$ data and are therefore not shown. As Fig. 8(a) shows, the magnetization oscillates about a stationary value for large values of H_z where the energy levels with different magnetization M are far separated in the energy-level diagram as we saw in Fig. 1. Let us study the c dependence of the saturated value $M_S=M_S(c)$. In Fig. 8(b), we plot the change in the magnetization $\Delta M/L=[M_S(c)-(-L)]/L$ as a function of $1/c$. As shown in Fig. 8(b), the data can be fitted well by the expression

$$\frac{\Delta M}{L} \simeq \frac{\Delta M_0}{L} + \frac{a}{c}, \tag{17}$$

where $\Delta M_0/L$ and a are constants. These constants, to good approximation, do not depend on the system size.

In order to explain the observed $1/c$ dependence, we present a perturbation scheme for fast sweeps (see Appendix B). We regard the sweeping-field (Zeeman) term as the zeroth-order system and treat the interaction among spins as the perturbation term. The result is a series expansion in terms of H_0/c [see Eq. (B8)], which explains the $1/c$ dependence.

In Appendix B, we also present a perturbation scheme based on independent Landau-Zener systems, each of which is given by a spin in a transverse field with a sweeping field. We show that this scheme can explain the behavior of the magnetization dynamics in the fast-sweep regime.

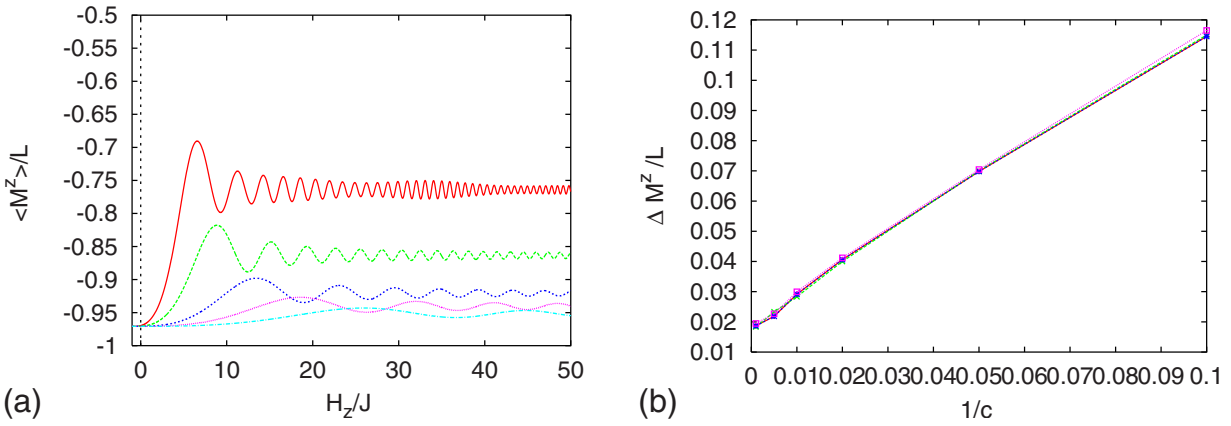

FIG. 8. (Color online) (a) The magnetization $M^z(t)$ as a function H_z for $L=12$, $H_x=0.7$, and various sweep velocities. Solid (red) line: $c=10$; long dashed (green) line: $c=20$; dashed (dark blue) line: $c=50$; dotted (magenta) line: $c=100$; and dashed dotted (cyan) line: $c=200$. (b) $\Delta M/L$ as a function of $1/c$ for $H_x=0.7$ and various system sizes. Solid (red) line: $L=4$; long dashed (green) line: $L=6$; dashed (dark blue) line: $L=10$; and dotted (magenta) line: $L=12$.

V. SUMMARY AND DISCUSSION

We have studied the time evolution of the magnetization in the ordered phase of the transverse Ising model under sweeping field H_z. We found significant jumps of the magnetization at a certain value of the magnetic field which we called quantum spinodal point H_z^{SP}. Although the energy-level diagram of the system significantly changes with the system size, we found size-independent magnetization processes for each pair (H_x,c).

In principle, it should be possible to understand the quantum dynamics of the magnetization from the energy-level diagram of the total system. Indeed the picture of successive Landau-Zener scattering processes works in slow-sweeping case.[3] However, for fast sweeps, the time evolution can be regarded as an assembly of local processes, with the interaction between the spins being a perturbation. Hence the dynamics of the magnetization does not depend on the size.

When the quantum fluctuations are weak (small H_x), a series of local spin flips governs the magnetization dynamics. The jumps of magnetization can be understood on the basis of energy-level crossings of certain spin clusters [Eq. (8)]. The energy-level structure corresponding to the local cluster flips is, of course, present in the energy-level diagram of the total system but it is hidden in the complicated structure of the huge number of energy levels.

For large values of H_x and fast sweeps, the magnetization process is also size independent. To explain this feature, we have presented a perturbation scheme in which the small parameter is H_0/c. In addition, we presented a perturbation scheme based of single-spin free Landau-Zener processes, which all together have allowed us to provide an understanding of the magnetization dynamics under field sweeps in terms of the energy-level structure.

ACKNOWLEDGMENTS

This work was partially supported by a Grant-in-Aid for Scientific Research on Priority Areas "Physics of new quantum phases in superclean materials" (Grant No. 17071011) and also by the Next Generation Super Computer Project, Nanoscience Program of MEXT. Numerical calculations were done on the supercomputer of ISSP.

APPENDIX A: SIZE DEPENDENCE OF THE ENERGY GAP AT $H_z=0$

The eigenvalues of model (1) are given by[9]

$$E = H_x \sum_q \omega_q (2\eta_q^\dagger \eta_q - 1), \tag{A1}$$

where η_q and $\eta_q^\dagger$ are fermion annihilation and creation operators, respectively, and

$$\omega_q = 2\sqrt{1 + 2\lambda \cos q + \lambda^2}, \tag{A2}$$

where $\lambda = J/H_x$. When the number of the fermions is even, q takes the values

$$q = \pm \frac{\pi}{L}, \pm \frac{3\pi}{L}, \ldots, \pm \frac{\pi(L-1)}{L} \tag{A3}$$

and when the number of the fermions is odd

$$q = 0, \pm \frac{2\pi}{L}, \pm \frac{4\pi}{L}, \ldots, \pm \frac{\pi(L-2)}{L}, \pi. \tag{A4}$$

Because $\omega_q > 0$, the ground state is given by $\eta_q^\dagger \eta_q = 0$. Thus, in the case of even number of fermions, the ground state is given by

$$E_{\mathrm{E1}} = -2H_x \sum_{m=1}^{L/2} \sqrt{1 + 2\lambda \cos\left(\frac{L-2m+1}{L}\right) + \lambda^2} \tag{A5}$$

and the first excited state is given by

$$E_{\mathrm{E2}} = E_{\mathrm{E1}} + 4H_x \sqrt{1 + 2\lambda \cos\left(\frac{L-1}{L}\right) + \lambda^2}. \tag{A6}$$

In the case of an odd number of fermions, the lowest-energy state is

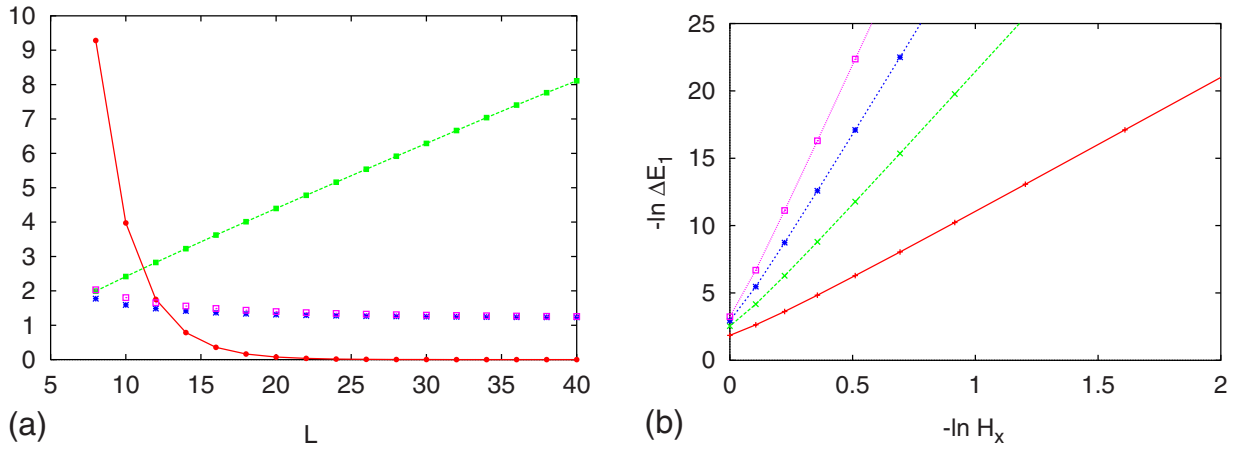

FIG. 9. (Color online) (a) Size dependence of the energy gaps for H_x=0.7. Bullets: difference $\Delta E_1/J(\times 500)$ between the energy of the first excited state and the ground-state energy. This difference vanishes exponentially with L. Solid squares: $-(\ln \Delta E_1/J)/2$; stars: $\Delta E_2/J$; and open squares: $\Delta E_3/J$. (b) The energy gap $\Delta E_1/J$ as a function of H_x for several L. Plus signs: L=10; crosses: L=20; stars: L=30; and open squares: L=40. Note the double-logarithmic scale. In both figures, lines are guides for the eyes only.

$$E_{O1} = H_x\sqrt{1+2\lambda+\lambda^2} + H_x\sqrt{1-2\lambda+\lambda^2} - 2H_x \sum_{m=1}^{L/2-1} \sqrt{1+2\lambda\cos\left(\frac{L-2m+1}{L}\right)+\lambda^2} \tag{A7}$$

and the first excited state is given by

$$E_{O2} = E_{O1} + 2H_x\sqrt{1-2\lambda+\lambda^2} + \sqrt{1+2\lambda\cos\left(\frac{L-2}{L}\right)+\lambda^2}. \tag{A8}$$

The energy gaps are given by

$$\Delta E_1 = E_{O1} - E_{E1}, \tag{A9}$$

$$\Delta E_2 = E_{E2} - E_{E1}, \tag{A10}$$

and

$$\Delta E_3 = E_{O2} - E_{E1}. \tag{A11}$$

Using these formulas, we can calculate the L dependence of the gaps. The results are plotted in Fig. 9(a). We find that ΔE_1 vanishes exponentially with L; that is,

$$\Delta E_1 \propto \exp(-aL), \tag{A12}$$

where a depends on λ. We also plot $-\log \Delta E_1/2$ to confirm the exponential dependence. On the other hand, we find that ΔE_2 is almost independent of L, and ΔE_3 is very close to ΔE_2, reflecting the fact that above the third level the infinite system has a continuous spectrum.

It is also of interest to study the dependence of the energy gap ΔE_1 on H_x for several L. In Fig. 9(b) we show the data on double-logarithmic scale. In the regime of small H_x we find a linear dependence on H_x, suggesting that

$$\Delta E_1 \propto H_x^{2S}. \tag{A13}$$

Indeed, for small H_x the slopes of the lines is given by $2S=L$. This dependence on H_x and L is to be expected when L spins flip simultaneously.

APPENDIX B: PERTURBATION ANALYSIS FOR LANDAU-ZENER-TYPE SWEEPING PROCESSES

When the sweep velocity c is very large, the duration of the sweep is very short. This suggests that it may be useful to study the magnetization processes by a perturbational method in terms of the small parameter $1/c$.

Let us consider the following model:

$$\mathcal{H} = \mathcal{H}_0 + ctV, \tag{B1}$$

where $\mathcal{H}_0$ and V are time independent. We will work in the interaction representation with respect to ctV; that is, we take the motion of ctV as reference, not $\mathcal{H}_0$ as is usually done. The Schrödinger equation is

$$i\hbar\frac{\partial}{\partial t}|\Psi\rangle = (\mathcal{H}_0 + ctV)|\Psi\rangle. \tag{B2}$$

In the interaction representation we have

$$|\Psi\rangle = e^{-ict^2V/2\hbar}|\Phi\rangle \tag{B3}$$

and the equation of motion is given by

$$i\hbar\frac{\partial}{\partial t}|\Psi\rangle = i\hbar(-ictV/\hbar)e^{-ict^2V/2\hbar}|\Phi\rangle + i\hbar e^{-ict^2V/2\hbar}\frac{\partial}{\partial t}|\Phi\rangle = e^{-ict^2V/2\hbar}\left(ctV + i\hbar\frac{\partial}{\partial t}\right)|\Phi\rangle, \tag{B4}$$

and therefore the Schrödinger equation for $|\Phi\rangle$ is given by

$$i\hbar\frac{\partial}{\partial t}|\Phi\rangle = e^{ict^2V/2\hbar}\mathcal{H}_0 e^{-ict^2V/2\hbar}|\Phi\rangle. \tag{B5}$$

Defining

$$W(t) \equiv e^{ict^2V/2\hbar}\mathcal{H}_0 e^{-ict^2V/2\hbar}, \tag{B6}$$

we can use the usual perturbation expansion scheme for

$$i\hbar\frac{\partial}{\partial t}|\Phi\rangle = W(t)|\Phi\rangle \tag{B7}$$

and find

$$|\Phi(t)\rangle = \left[1 + \left(\frac{1}{i\hbar}\right)\int_{t_0}^{t} W(t_1)dt + \left(\frac{1}{i\hbar}\right)^2 \times \int_{t_0}^{t}\int_{t_0}^{t_1} W(t_1)W(t_2)dt_1dt_2 + \cdots\right]|\Phi(0)\rangle. \tag{B8}$$

In the sweep $(-H_0 < ct < H_0)$, $t_0 = -H_0/c$ and $t = H_0/c$. Thus, the integral is of order the H_0/c. Therefore we can regard the above expansion as a series expansion in terms of power of H_0/c. Of course the series can be also regarded as a power of $\mathcal{H}_0$ as in the usual sense.

1. Transverse Ising model under a field sweep

Now, we consider our problem

$$\mathcal{H}(t) = -J\sum_j \sigma_j^z\sigma_{j+1}^z - H_x\sum_j \sigma_j^x - ct\sum_j \sigma_j^z. \tag{B9}$$

We set

$$\mathcal{H}_0 = -J\sum_j \sigma_j^z\sigma_{j+1}^z - H_x\sum_j \sigma_j^x \tag{B10}$$

and

$$V = -\sum_j \sigma_j^z. \tag{B11}$$

Then, $W(t)$ is given by

$$W(t) = \exp\left(-ict^2/2\hbar\sum_j \sigma_j^z\right)\mathcal{H}_0 \exp\left(ict^2/2\hbar\sum_j \sigma_j^z\right) = -J\sum_j \sigma_j^z\sigma_{j+1}^z - H_x\sum_j (\sigma_j^+ e^{-ict^2/\hbar} + \sigma_j^- e^{ict^2/\hbar}). \tag{B12}$$

We may include the diagonal term $-J\Sigma_j\sigma_j^z\sigma_{j+1}^z$ in V. Then the expansion is regarded as series of H_x. This expansion corresponds to the series of jumps discussed in Eq. (8).

We also note that if $J=0$ the above process is an ensemble of independent Landau-Zener processes. Each of them is independently expressed by

$$i\hbar\frac{\partial}{\partial t}|\Phi_{\mathrm{LZ}}(t)\rangle = -H_x(\sigma^+ e^{-ict^2/\hbar} + \sigma^- e^{ict^2/\hbar})|\Phi_{\mathrm{LZ}}(t)\rangle. \tag{B13}$$

2. Perturbation theory in terms of independent LZ systems

Next, we consider the case in which the transverse field is included in V. We sweep the field from $-H_0$ to H_0. The duration of the sweep is $2H_0/c$. We assume that

$$H_0 \gg J > H_x, \tag{B14}$$

such that the motion due to V is that of an ensemble of independent Landau-Zener processes. Thus, we consider the ensemble of the LZ systems as the unperturbed system.

We know the properties of each system. Namely, we know that the scattering becomes small when c becomes large. The time evolution of each LZ system is given by

$$\begin{pmatrix}1\\0\end{pmatrix} \to e^{i\phi(t)}\begin{pmatrix}\sqrt{p}\\ \sqrt{1-p}e^{i\varepsilon(t)}\end{pmatrix} \equiv \psi(t), \tag{B15}$$

in the adiabatic basis—that is, in the representation that uses the eigenstates of the system with given $H_z(t)$. Here, p is the probability for staying the ground state. In the Landau-Zener theory, p is given by the well-known expression

$$p = 1 - \exp\left(-\frac{\pi H_x^2}{\hbar c}\right). \tag{B16}$$

In the case of small H_0, p may have a different form. Even in those cases, expression (B15) is still correct and the present formulation works if we employ a correct expression for p.

The unperturbed state is given by

$$\Phi_0(t) = \prod_j \psi_j(t) = e^{iL\phi(t)}\begin{pmatrix}\sqrt{p}\\ \sqrt{1-p}\,e^{i\varepsilon(t)}\end{pmatrix}_1 \otimes \begin{pmatrix}\sqrt{p}\\ \sqrt{1-p}\,e^{i\varepsilon(t)}\end{pmatrix}_2 \otimes \cdots \otimes \begin{pmatrix}\sqrt{p}\\ \sqrt{1-p}\,e^{i\varepsilon(t)}\end{pmatrix}_L. \tag{B17}$$

The zeroth order is given a usual Landau-Zener process of which the energy diagram is given by Fig. 10(a), which shows the energy-level diagram for the two independent spins. Thus, in this case there are four states (++), (+−), (−+), and (−−). The states consisting of (+−) and (−+) are degenerate with energy zero.

The interaction term $-J\Sigma_j\sigma_j^z\sigma_{j+1}^z$ is the perturbation. As long as expansion (B8) converges with less than Lth terms, it gives a local effect. To the first order in J, only the nearest-neighbor spins interact, giving a contribution of the order J. The sweep-velocity dependence is taken into account through the zeroth-order term. If we take a large H_0, the integral in Eq. (B8) is no longer small, and we have to regard Eq. (B8) as a series of J. Therefore, we do not have any small parameter and Eq. (B8) represents the original general dynamics. In the case of fast sweeps, the effective range of quantum mixing in which the diabatic energy levels (levels for $H_x=0$) cross each other is of the order $L\times J$, and therefore the duration of interaction is of the order LJ/c. Hence, the integration gives a contribution of the order LJ/c which now becomes the small parameter. In the case of finite H_0, the small parameter is the minimum of $(H_0/c, LJ/c)$. In the present study, $H_0=1$. Then H_0/c is the small parameter and we cannot use the form of p given in Eq. (B16). In any case, the series converges for the fast sweeps and we expect that the perturbation effect does not depend on L.

The system described by the first-order perturbation theory corresponds to a Hamiltonian of two spins exhibiting

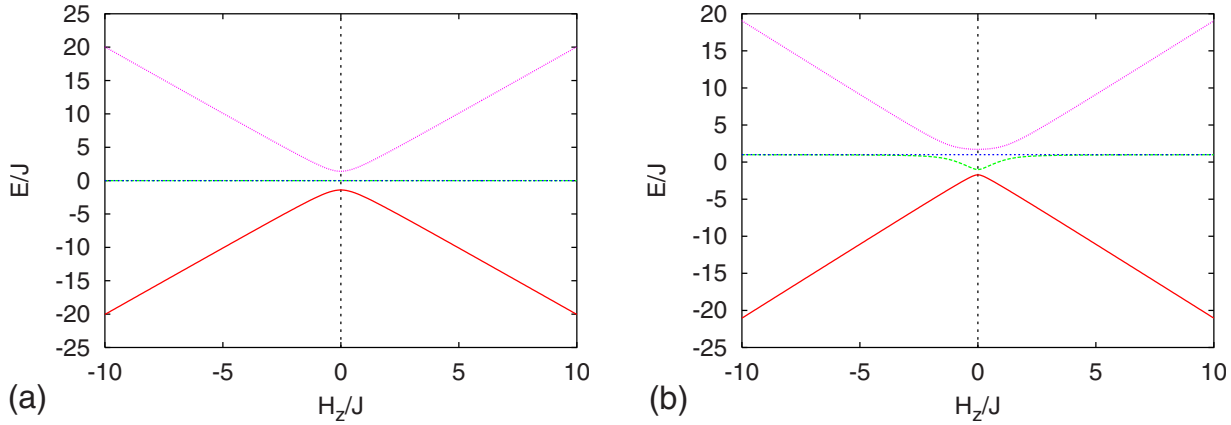

FIG. 10. (Color online) Energy-level diagram for a two-spin Landau-Zener model (B18) with $H_x=0.7$. (a) $J=0$ and (b) $J=1$.

the Landau-Zener scattering process and which are coupled by an Ising interaction. The Hamiltonian reads

$$\mathcal{H}_{\mathrm{CLZ}} = -J\sigma_1^z\sigma_2^z - (H_x\sigma_1^x - ct\sigma_1^z) - (H_x\sigma_2^x - ct\sigma_2^z). \tag{B18}$$

The energy-level diagram of this system is shown in Fig. 10(b). Let us study the effect of the interaction on the dynamics in this case. We compare the magnetization processes of model (B18) with $J=0$ and $J=1$. The results are shown in Fig. 11(a). Note that the sweep starts from $H_z=-H_0=-1$.

Next, in Fig. 11(b), we show the magnetization processes for $c=100$ for model (B18) with that of the same model with J replaced with $2J$. If we use a small value of H_0, the ground states of the models at $H_z=-1$ differ significantly. Therefore, to compare the results, in this figure, we take $H_0=-60$ such that the ground state of both models is close to the all-spin-down state. The average of the first and the third curves is close to the second curve. This fact indicates that the processes are well described by the first-order perturbation theory. Indeed, the deviation from the single Landau-Zener model is 0, J, and $2J$, respectively.

We also compare the magnetization processes of model (B18) with J replaced with $2J$ and that of a model with three spins in Fig. 12(a). The difference between the models of four spins and of 12 spins is also shown in Fig. 12(b). In all these cases, we start at $H_z=-1$ because the magnetizations per spin are very close in all the cases. We find almost no difference, indicating that the processes are well described by the first-order perturbation theory.

When the sweep velocity becomes small, we may need higher-order perturbation terms. If the relevant order of the perturbation is less than the length of the chain, we expect a size-independent magnetization process. The size-independent magnetization in the quantum spinodal decomposition can be understood in this way.

The local motion of magnetization can be understood from a view point of an effective field from the neighboring spins. We may study the magnetization process of a single spin in a dynamical mean-field generated by its neighbors.[17]

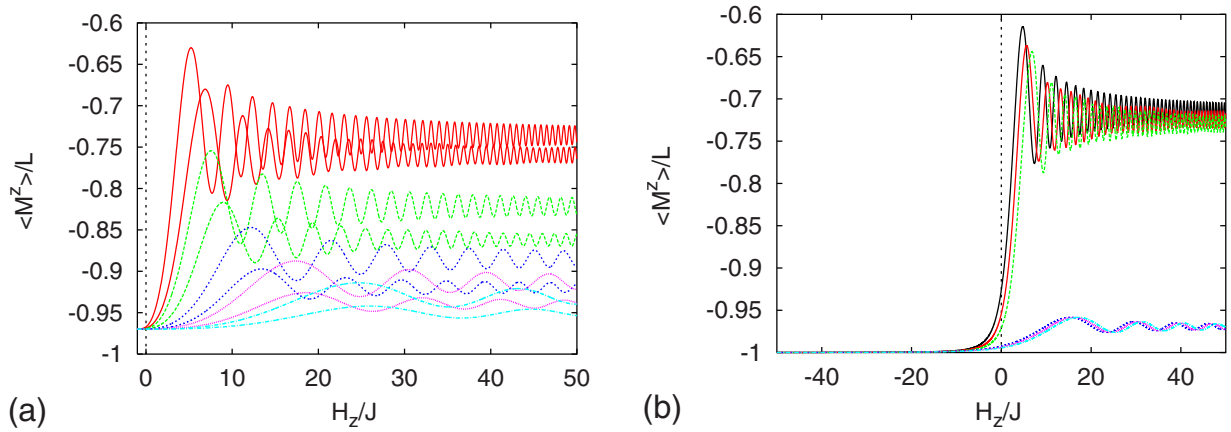

FIG. 11. (Color online) (a) Comparison of the magnetization processes of model (B18) with $J=0$ (thin line) and $J=1$ (thick lines) for $H_x=0.7$. Solid (red) line: $c=10$; long dashed (green) line: $c=20$; dashed (dark blue) line: $c=50$; dotted (magenta) line: $c=100$; and dashed-dotted (cyan) line: $c=200$. For each c, the magnetization of the single LZ process is shifted by an amount such that at $H_z=-1$ it coincides with the magnetization of model (B18) with J replaced with $2J$. (b) Comparison of the magnetization of a single LZ process that of model (B18) and that of model (B18) with J replaced with $2J$. $H_x=0.7$ and $c=100$. Solid (black) line: $c=10$, single LZ process; solid (red) line: $c=10$, Eq. (B18); long dashed (green) line: $c=10$, Eq. (B18) with J replaced with $2J$; dashed (dark blue) line: $c=100$, single LZ process; dotted (magenta) line: $c=100$, Eq. (B18); and dashed-dotted (cyan) line: $c=100$, Eq. (B18) with J replaced with $2J$.

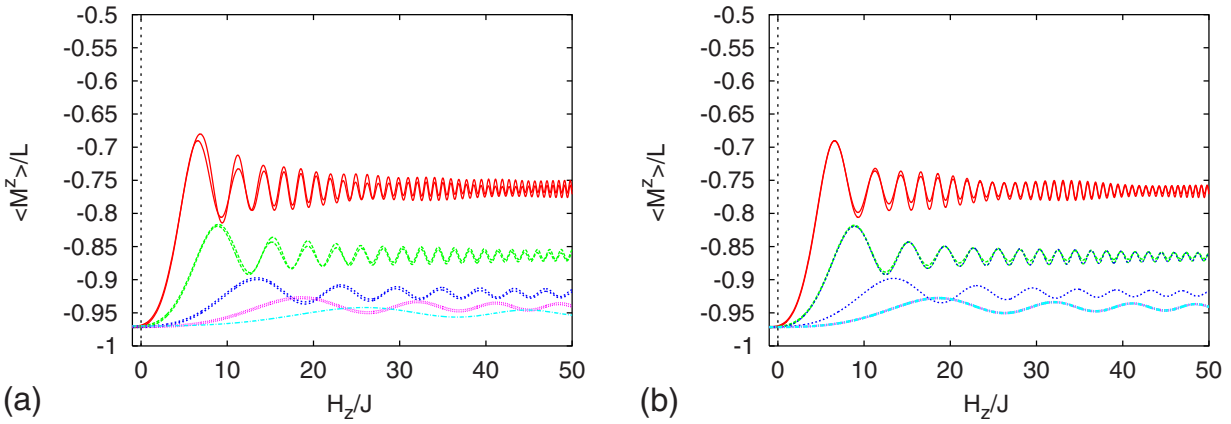

FIG. 12. (Color online) (a) Comparison of the magnetization processes of model (B18) with J replaced with $2J$ (thin lines) and the model with three spins (thick lines) for $H_x=0.7$. Solid (red) line: $c=10$; long dashed (green) line: $c=20$; dashed (dark blue) line: $c=50$; dotted (magenta) line: $c=100$; and dashed-dotted (cyan) line: $c=200$. (b) Same as left except that the comparison is between models with $L=4$ (thin lines) and $L=12$ (thick lines) for $H_x=0.7$.

Let us describe the situation by the following Hamiltonian:

$$\mathcal{H}_{\mathrm{MF}} = -[H_z(t) + 2J\langle\sigma^z\rangle]\sigma^z - H_x\sigma^x. \tag{B19}$$

Because the mean field is almost $2J$ during the fast sweep, the mean field simply shifts H_0 by a constant $2J$. Thus, we conclude that for fast sweeps, the dynamics is very similar to that of a single spin, meaning that, for the dynamics, the effective field on each spin in the lattice is essentially that same as the applied field. This conclusion is consistent with our earlier comparison of the zeroth- and first-order perturbation results.

*Corresponding author; miya@spin.phys.s.u-tokyo.ac.jp

[1] C. Zener, Proc. R. Soc. London, Ser. A **137**, 696 (1932); L. Landau, Phys. Z. Sowjetunion **2**, 46 (1932); E. C. G. Stückelberg, Helv. Phys. Acta **5**, 3207 (1932).

[2] S. Miyashita, J. Phys. Soc. Jpn. **64**, 3207 (1995); S. Miyashita, *ibid.* **65**, 2734 (1996).

[3] H. De Raedt, S. Miyashita, K. Saito, D. Garcia-Pablos, and N. Garcia, Phys. Rev. B **56**, 11761 (1997).

[4] D. Gatteschi, R. Sessoli, and J. Villain, *Molecular Nanomagnets* (Oxford University Press, New York, 2006).

[5] L. Thomas, F. Lionti, R. Ballou, D. Gatteschi, R. Sessoli, and B. Barbara, Nature (London) **383**, 145 (1996); J. R. Friedman, M. P. Sarachik, J. Tejada, and R. Ziolo, Phys. Rev. Lett. **76**, 3830 (1996); J. A. A. J. Perenboom, J. S. Brooks, S. Hill, T. Hathaway, and N. S. Dalal, Phys. Rev. B **58**, 330 (1998); T. Kubo, T. Goto, T. Koshiba, K. Takeda, and K. Awaga, *ibid.* **65**, 224425 (2002); C. Sangregorio, T. Ohm, C. Paulsen, R. Sessoli, and D. Gatteschi, Phys. Rev. Lett. **78**, 4645 (1997).

[6] I. Chiorescu, W. Wernsdorfer, A. Müller, H. Bögge, and B. Barbara, Phys. Rev. Lett. **84**, 3454 (2000); I. Rousochatzakis, Y. Ajiro, H. Mitamura, P. Kogerler, and M. Luban, *ibid.* **94**, 147204 (2005); En-Che Yang, W. Wernsdorfer, L. N. Zakharov, Y. Karaki, A. Yamaguchi, R. M. Isidro, G.-D. Li, S. A. Willson, A. L. Rheingold, H. Ishimoto, and D. N. Hendrickson, Inorg. Chem. **45**, 529 (2006); K.-Y. Choi, Y. H. Matsuda, H. Nojiri, U. Kortz, F. Hussain, A. C. Stowe, C. Ramsey, and N. S. Dalal, Phys. Rev. Lett. **96**, 107202 (2006); S. Bertaina, S. Gambarelli, T. Mitra, B. Tsukerblat, A. Müller, and B. Barbara, Nature (London) **453**, 203 (2008).

[7] W. Wernsdorfer and R. Sessoli, Science **284**, 133 (1999); M. Ueda, S. Maegawa, and S. Kitagawa, Phys. Rev. B **66**, 073309 (2002).

[8] M. Suzuki, Prog. Theor. Phys. **58**, 755 (1977).

[9] B. K. Chakrabati, A. Dutta, and P. Sen, *Quantum Ising Phase and Transverse Ising Models* (Springer, Heidelberg, 1996).

[10] Y. Oshima, H. Nojiri, K. Asakura, T. Sakai, M. Yamashita, and H. Miyasaka, Phys. Rev. B **73**, 214435 (2006); J. Kishine, T. Watanabe, H. Deguchi, M. Mito, T. Sakai, T. Tajiri, M. Yamashita, and H. Miyasaka, *ibid.* **74**, 224419 (2006); W. Wernsdorfer, R. Clérac, C. Coulon, L. Lecren, and H. Miyasaka, Phys. Rev. Lett. **95**, 237203 (2005).

[11] T. Kadowaki and H. Nishimori, Phys. Rev. E **58**, 5355 (1998); A. Das and B. K. Chakrabarti, *Quantum Annealing and Related Optimization Methods*, (Springer, New York, 2005); G. E. Santoro and E. Tosatti, J. Phys. A **39**, R393 (2006); A. Das and B. K. Chakrabarti, Rev. Mod. Phys. **80**, 1061 (2008); S. Morita and H. Nishimori, J. Phys. A **39**, 13903 (2006); J. Phys. Soc. Jpn. **76**, 064002 (2007).

[12] J. Dziarmaga, Phys. Rev. Lett. **95**, 245701 (2005).

[13] T. W. B. Kibble, J. Phys. A **9**, 1387 (1976); Phys. Rep. **67**, 183 (1980); W. H. Zurek, Nature (London) **317**, 505 (1985); Phys. Rep. **276**, 177 (1996).

[14] V. V. Dobrovitski and H. A. De Raedt, Phys. Rev. E **67**, 056702 (2003).

[15] K. Saito, S. Miyashita, and H. De Raedt, Phys. Rev. B **60**, 14553 (1999).

[16] E. C. Stoner and E. P. Wohlfarth, Philos. Trans. R. Soc. London, Ser. A **240**, 599 (1948).

[17] A. Hams, H. De Raedt, S. Miyashita, and K. Saito, Phys. Rev. B **62**, 13880 (2000).